

Selective enhancement of Coulomb interactions in planar Weyl fermions

Vadym Apalkov^a, Wenchen Luo^b, and Tapash Chakraborty^c

^a*Department of Physics and Astronomy, Georgia State University,
Atlanta, Georgia, 30303, USA,* ^b*School of Physics,*

Central South University, Changsha, Hunan 410083, China,

^c*Department of Physics and Astronomy, University of Manitoba, Winnipeg, MB, Canada*

(Dated: January 27, 2025)

We report on our study of the electron interaction effects in topological two-dimensional (2D) materials placed in a quantizing magnetic field. Taking our cue from a recent experimental report, we consider a particular case of bismuthene monolayer with a strong spin-orbit interaction which can be a Weyl semimetal when placed on a specially tuned substrate. Interestingly, we observe that in some Landau levels of this material, the interaction effects are strongly enhanced compared to those for a conventional 2D system. Such an enhancement of electron-electron interactions in these materials is largely due to an anisotropy present in the materials. Additionally, the interaction effects can be tuned by changing the coupling to the substrate and the strongest inter-electron interactions are observed when the system is a Weyl semimetal. The observed enhancement of the interaction effects can therefore be an important signature of the 2D Weyl fermions.

Discovery of the integer quantum Hall effect (IQHE) in 1980, which originated in uniform two-dimensional (2D) electron gas in a perpendicular high magnetic field [1], ushered in a new era of condensed matter physics [2]. Subsequently, it was realized that this effect can also in principle be associated with a topological invariant of 2D band structure, the Chern number [3], that can be interpreted in terms of the Berry curvature [4]. Soon after the discovery of IQHE, fractional quantum Hall effect (FQHE) was discovered [5, 6], and the origin of that remarkable effect was explained as a direct result of strong electron-electron interactions [7]. Those interactions lead to a unique incompressible state [8], where the fractionally-charged low-energy quasiparticles obey exotic fractional statistics [2, 9, 10]. The incompressible state was also found to display many other important physical properties [8, 11–14], and exploration of interacting 2D electron gas dominated research in condensed matter physics. However, research on electronic states took a dramatic turn after successful fabrication of graphene [2, 15] and topological insulators [16] when the low-energy dynamics of 2D electrons were found to obey the Dirac equation, rather than the usual Schrödinger equation and soon the concepts of topology and chirality driven electronic properties came to the fore. The age of exploration of quantum materials then began in earnest [17]. For interacting Dirac fermions, many-body interaction-driven properties, such as the FQHE, were found to be present in monolayer, bilayer and double-layer graphene systems [18–23], and in topological insulators [24]. The next major advancement in search of topological materials was finding the Weyl fermions, the zero-mass solution of the Dirac equation, in condensed matter systems [25] and the properties of topological semimetals [26, 27] received serious attention. Here also a new milestone was achieved in 2024 when the 2D Weyl semimetals were reported [28].

Electronic states of topological quantum materials in 2D have the clear advantage over their three-dimensional

counterparts because they are easily manipulated by the externally applied fields. While research in quantum materials has been largely based on the non-trivial topological properties of the electronic bands, a microscopic approach to the interaction-induced many-body properties is important to fully understand the intricacies of these novel materials. The advantages of having Weyl semimetals in reduced dimensions are manifold: in addition to their new physical characteristics, they can be easily integrated in devices of low-dimensions, and the theoretical techniques developed for decades to investigate other low-dimensional systems can possibly be applied here as well (with suitable modifications).

In this work, we report on the quantizing magnetic field induced properties of interacting Weyl fermions in two dimensions. We found several unconventional features in the system. More specifically, we analyze a special case of bismuthene monolayer [28], which in a free-standing case behaves as gapped anisotropic graphene-like material, where the gap is determined by the spin-orbit interaction, but on a specially chosen substrate, e.g., the SnSe substrate, it becomes a Weyl semimetal. When such a system is placed in a quantizing magnetic field, we find several remarkable features: an enhancement of electron-electron interactions within a single Landau level compared to a conventional two-dimensional materials. This enhancement is largely due to the anisotropy present in the system, which results in the system's Landau levels that are the mixtures of the conventional 2D Landau levels. When the bismuthene monolayer is placed on a substrate, which breaks the inversion symmetry and produced a Weyl semimetal with two valleys, the electron-electron interactions become even more enhanced in one of the valleys of the system.

As mentioned above, the system of two dimensional Weyl semimetal adopted here has been realized in bismuthene monolayer placed on a SnSe substrate [28]. The substrate breaks the inversion symmetry of the system and results in the formation of two Weyl points with

low-energy linear dispersion. Near the Weyl points the low-energy effective electron Hamiltonian takes the form

$$\mathcal{H}_\tau = \tau (v_x k_x \sigma_x + \Delta k_x) + v_y k_y \sigma_y + \tau \lambda_{SOC} \sigma_z s_z + \lambda_S \sigma_z, \quad (1)$$

where σ_i and s_i are Pauli matrices corresponding to sublattice and spin degrees of freedoms, respectively. The system has the following parameters: Fermi velocities along the x and y directions, $v_x = 3.17 \times 10^5$ m/s, $v_y = 4.23 \times 10^5$ m/s, tilting of the Weyl cone in the k_x direction, $\Delta = 0.19 \times 10^5$ m/s, and the spin-orbit coupling, $\lambda_{SOC} = 55$ meV. Coupling of bismuthene monolayer to the substrate introduces the term $\lambda_S \sigma_z$, which breaks the inversion symmetry and if $\lambda_S = \lambda_{SOC}$ then the energy dispersion is gapless with two Weyl points which are labeled by the parameter $\tau = \pm 1$. In what follows, we consider λ_S as a variable parameter of the system, which can be controlled by using different substrates. The anisotropy of the system is determined by the difference between the Fermi velocities, v_x and v_y , and by the parameter Δ , which characterizes the tilting of the Weyl cones. The important role that the anisotropy plays in our system will soon be clear below.

In the presence of a magnetic field B perpendicular to the bismuthene monolayer, the electron momentum is replaced with $\pi = \mathbf{p} - e\mathbf{A}$, where \mathbf{A} is the corresponding vector potential. In the symmetric gauge, the vector potential is $\mathbf{A} = (-By/2, Bx, 0)$. Then the Landau levels can be calculated by expressing the corresponding wave functions in the bases of Landau functions $\phi_{n,m}$ of the conventional electron system with parabolic energy dispersion, where n is the corresponding Landau level index and m is the z component of the angular momentum. Below we consider only one component of the electron spin, say $s_z = -1$, assuming that the levels of the system with different spin components are separated by the Zeeman energy. Therefore, for a given spin component, the Landau level wavefunctions can be expressed as

$$\Psi_{n,m} = \begin{pmatrix} \sum_{n_1} C_{n,n_1} \phi_{n_1,m} \\ \sum_{n_1} D_{n,n_1} \phi_{n_1,m} \end{pmatrix}, \quad (2)$$

where C_{n,n_1} and D_{n,n_1} are unknown coefficients which can be found from solutions of the corresponding eigenvalue equation $\mathcal{H}_\tau \Psi_{n,m} = E_n \Psi_{n,m}$ and E_n is the Landau energy spectrum. In the expansion, Eq. (2), of the wavefunctions $\Psi_{n,m}$ in terms of conventional Landau level functions $\phi_{n,m}$ we consider a finite number of functions $\phi_{n,m}$, $n = 0, \dots, N$. Then, for a given Weyl point $\tau = \pm 1$, the size of the corresponding Hamiltonian matrix \mathcal{H}_τ is $2(N+1)$. From diagonalization of such a matrix, we obtain the Landau energy spectrum, E_n , and the coefficients C_{n,n_1} and D_{n,n_1} . In our studies below, we consider $N = 100$.

The electron-electron interaction within a single Landau level is characterized in terms of the Haldane pseudopotentials, V_m , which are the energies of the interaction of two electrons with relative angular momentum m [29]. With the known Landau level wavefunctions (2),

the Haldane pseudopotentials have the following form

$$V_m^{(n)} = \sum_{n_1, n_2} (C_{n,n_1}^* C_{n,n_2} + D_{n,n_1}^* D_{n,n_2}) \times \int_0^\infty \frac{dq}{2\pi} q V(q) L_{n_1}(q^2/2) L_{n_2}(q^2/2) L_m(q^2) e^{-q^2}, \quad (3)$$

where $V(q) = \frac{e^2}{\epsilon l_B q}$ is the Coulomb interaction in the momentum space, l_B is the magnetic length, e is the electron charge, ϵ is the dielectric constant, and $L_n(x)$ are the Laguerre polynomials.

The Landau levels of the bismuthene monolayer are shown in Fig. 1 for two values of λ_S , corresponding to the case of free standing bismuthene monolayer, $\lambda_S = 0$ [Fig. 1(a)] and a monolayer on a substrate with $\lambda_S = \lambda_{SOC}$ [Fig. 1(b)]. The results are shown for two Weyl points, i.e., for $\tau = \pm 1$. For the case of $\lambda_S = 0$, without the magnetic field, the system has a bandgap of $2\lambda_{SOC}$, which is also clearly visible in the corresponding Landau spectrum. For $\lambda_S = \lambda_{SOC}$, the gap is closed and the Weyl semimetal is realized. In this case, for one of the Weyl point, $\tau = 1$, i.e., for one of the valleys, the Landau spectrum shows the gapless behavior with one of the levels having zero energy, while for the other valley, $\tau = -1$, the Landau energy spectrum shows a finite gap with the value of $4\lambda_{SOC}$. In both panels, the Landau levels with the strongest electron-electron interactions, i.e., the largest values of the corresponding Haldane pseudopotentials, are shown by red lines. The levels are marked as L_1 and L_2 [Fig. 1].

The Haldane pseudopotentials, V_m , for a few Landau levels of the system are shown in Fig. 2. The largest pseudopotentials are realized at the Landau levels L_1 and L_2 , which are marked by red dots in Fig. 2. We also show the Haldane pseudopotentials for a conventional electron system with parabolic energy dispersion for the Landau level $n = 0$ by green dots. The data in Fig. 2 show that electron-electron interactions are strongly enhanced for a bismuthene monolayer compared to the conventional case. Also, the strongest electron-electron interactions are realized for the Landau level L_1 for the case of the Weyl semimetal [Fig. 2(b)] when $\lambda_S = \lambda_{SOC}$.

One of the characteristic features of electron-electron interactions is how fast the corresponding Haldane pseudopotentials decay with increasing relative angular momentum, m . Such a decay determines the stability of the FQHE states and is characterized by the ratio of Haldane pseudopotentials, V_i/V_j , for example, V_0/V_1 , V_1/V_3 , and V_3/V_5 . These ratios are shown in Fig. 3 as a function of the magnetic field. For a free-standing bismuthene monolayer [Fig. 3(a)] the results are the same for both L_1 and L_2 Landau levels. The ratio V_0/V_1 shows a monotonic increase with the magnetic field, while both V_1/V_3 and V_3/V_5 are saturated at a magnetic field of around 1 T and remain constant for $B > 1$ T. The corresponding saturated values are greater than the corresponding ratios for the conventional case at Landau level $n = 0$, which are shown by green arrows.

In the case of the Weyl semimetal [Fig. 3(b)] which corresponds to the condition of $\lambda_S = \lambda_{SOC}$, the results for the Landau levels L_1 and L_2 are different and the corresponding ratios show very different behaviors. For the L_2 Landau level, the pseudopotentials do not depend on the magnetic field due to effective cancellation of a spin-orbit term in the Hamiltonian (1) by the substrate coupling, i.e., $\lambda_S - \lambda_{SOC} = 0$ for $\tau = -1$. For the L_1 Landau level, the ratios V_1/V_3 and V_3/V_5 as a function of the magnetic field are constant for $B > 2$ T, but V_0/V_1 monotonically increases with B . While V_3/V_5 for both

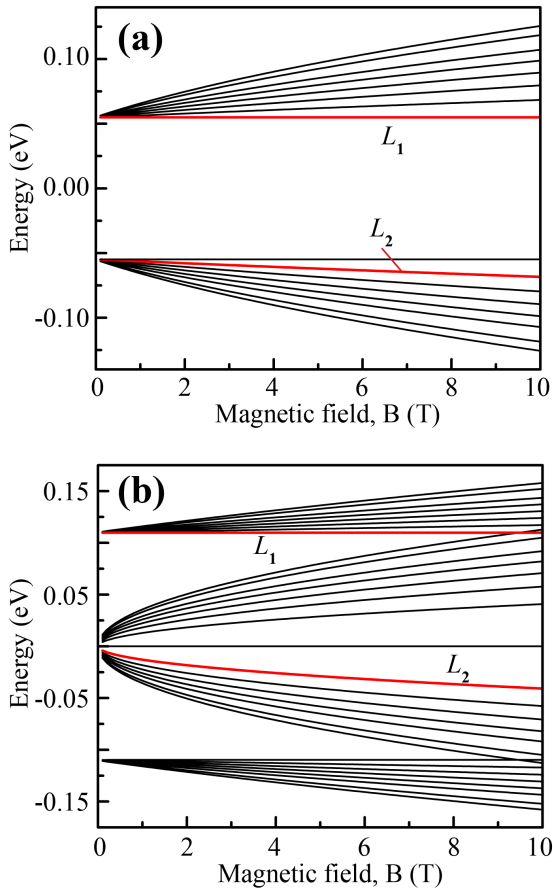


FIG. 1. Landau levels of a bismuthene monolayer with two values of substrate coupling, λ_S : (a) $\lambda_S = 0$, which corresponds to free-standing monolayer, (b) $\lambda_S = \lambda_{SOC} = 55$ meV, which corresponds to the Weyl semimetal case. The results are shown for only one component of electron spin, $s_z = -1$. The red lines show the Landau levels with strong electron-electron coupling. Such a coupling is characterized by the corresponding Haldane pseudopotentials. The Landau levels with strong electron-electron coupling are labeled as L_1 and L_2 levels. Two sets of Landau levels correspond to two Weyl points, $\tau = \pm 1$, where the set of Landau levels, which is originated from the spectrum with zero bandgap, corresponds to the Weyl point $\tau = 1$, while another set, with a finite bandgap, corresponds to the Weyl point $\tau = -1$.

Landau levels, L_1 and L_2 , are almost the same, the ratio V_1/V_3 for the Landau level L_1 is much larger than the one for the level L_2 .

To examine the properties of the system as the coupling of a bismuthene monolayer to the substrate changes from the free-standing case to the Weyl semimetal, we plot the first few Haldane pseudopotentials and the corresponding ratios as a function of λ_S in Fig. 4. The results are shown for both L_1 and L_2 Landau levels. In Fig. 4(a), the pseudopotentials V_0 , V_1 , V_3 , and V_5 are presented. For $\lambda_S = 0$, the values of these pseudopotentials are the same for L_1 and L_2 Landau levels. With increasing λ_S , the pseudopotentials monotonically increase and decrease for levels L_1 and L_2 , respectively. The only small deviation from this behavior is for the pseudopotentials V_3 and V_5 , which for the Landau level L_2 shows a local minimum at $\lambda_S \approx 0.045$ eV. The behavior of pseudopotentials shown in Fig. 4(a) suggest that with increasing λ_S , i.e., by increasing the coupling to the substrate, the electron-electron interactions are enhanced for the Landau level L_1 but are suppressed for the Landau level L_2 . To further illustrate this property we evaluate the $\nu = 1/3$ -FQHE energy gaps, $\Delta_{1/3}$ [8], for different values of λ_S . The calculations were done in the spherical geometry with seven electrons in the system and the magnetic field of 2 T. When $\lambda_S = 0$, for both L_1 and L_2 levels, the gap is around $\Delta_{1/3} \approx 0.148\epsilon_C$, where $\epsilon_C = e^2/\epsilon l_B$ is the Coulomb energy. With increasing λ_S , the gap $\Delta_{1/3}$ monotonically increases for the L_1 level and reaches the value of $0.19\epsilon_C$ at $\lambda_S = \lambda_{SOC}$. For the L_2 level, the gap $\Delta_{1/3}$ monotonically decreases with λ_S and becomes $0.067\epsilon_C$ at $\lambda_S = \lambda_{SOC}$. It is worth noting that in all the cases, the gaps are considerably larger than that of the $1/3$ -FQHE in conventional semiconductors or graphene which is about $0.07\epsilon_C$ [18].

The ratios of the pseudopotentials, V_m , are also shown in Fig. 4 as a function of λ_S . For the level L_1 , the ratios show a monotonic dependence on λ_S , where both V_0/V_1 and V_1/V_3 monotonically decrease with λ_S , while V_3/V_5 remains almost constant. For the level L_2 , the ratios V_0/V_1 and V_1/V_3 show a non-monotonic dependence on λ_S with local maxima at ≈ 0.03 eV and at ≈ 0.045 eV. The selective enhancement of interaction effects is therefore manifestly clear from these results.

We also note that the electron-electron interaction effects in three-dimensional (3D) Weyl semimetals were reported in Refs. [30–32], where the interactions opened a bandgap in the single-particle energy spectrum under a special population of the energy levels in such 3D systems. The bandgaps are opened either in the magnetic 3D Weyl semimetals[30, 31] or in 3D Weyl semimetals placed in an external magnetic field[32]. Under these conditions the FQHE with fractional quantization of the Hall conductance can be realized in these Weyl semimetals. The fundamental difference between these results and those of ours is that our system is purely two dimensional, which results in the formation of discrete single-particle Landau level spectrum, while in Refs. [30–32]

the Weyl systems are three dimensional with continuous single-particle energy spectra.

There are multitude of possible reasons behind the selective enhancement of electron-electron interactions at some Landau levels of the system that is discussed above. One of the most likely scenarios is the anisotropy of the system, which in Weyl semimetal systems can sometimes result in some unusual reported effects, such as the chiral anomaly, which is associated with a variety of unusual anisotropic magnetoresistance[33, 34], and a change in the nature of the density of states etc. [35]. In our case, the anisotropy present in the bismuthene monolayer results in Landau levels that are the mixtures of conventional two-dimensional Landau levels. Such a mixture changes the effective electron-electron interactions within a given Landau level and for some of them, it actually enhances the interactions between electrons compared to the conventional case. The unusual behavior of different Landau levels associated with the energy gaps that we have found here might be a signature of the 2D Weyl

fermions considered here. From a broader perspective, our present study indicates the possible route to investigate the interaction effects in low-dimensional topological materials, by the application of a quantizing magnetic field.

ACKNOWLEDGMENTS

Major funding was provided by Grant No. DE-FG02-01ER15213 from the Chemical Sciences, Biosciences, and Geosciences Division, Office of Basic Energy Sciences, Office of Science, US Department of Energy. Numerical simulations were performed using support by Grant No. DE-SC0007043 from the Materials Sciences and Engineering Division of the Office of the Basic Energy Sciences, Office of Science, US Department of Energy, and was supported in part by the High Performance Computing Center of Central South University.

-
- [1] K. von Klitzing, T. Chakraborty, P. Kim, V. Madhavan, X. Dai, J. McIver, Y. Tokura, L. Savary, D. Smirnova, A. M. Rey, C. Felser, J. Gooth, and X. Qi, 40 years of the quantum hall effect, *Nature Reviews Physics* **2**, 397 (2020).
- [2] T. Chakraborty, ed., Introduction, in *Encyclopedia of Condensed Matter Physics (Second Edition)* (Academic Press, Oxford, 2024) pp. ix–xvii.
- [3] D. J. Thouless, M. Kohmoto, M. P. Nightingale, and M. den Nijs, Quantized hall conductance in a two-dimensional periodic potential, *Physical Review Letters* **49**, 405 (1982).
- [4] B. Simon, Holonomy, the quantum adiabatic theorem, and berry’s phase, *Physical Review Letters* **51**, 2167 (1983).
- [5] D. C. Tsui, H. L. Stormer, and A. C. Gossard, Two-dimensional magnetotransport in the extreme quantum limit, *Physical Review Letters* **48**, 1559 (1982).
- [6] H. L. Störmer, Two-dimensional electron correlation in high magnetic fields, *Physica B: Condensed Matter* **177**, 401 (1992).
- [7] R. B. Laughlin, Anomalous quantum hall effect: An incompressible quantum fluid with fractionally charged excitations, *Physical Review Letters* **50**, 1395 (1983).
- [8] T. Chakraborty and P. Pietiläinen, *The Fractional Quantum Hall Effect* (Springer, New York, 1988).
- [9] M. Greiter and F. Wilczek, Fractional statistics, *Annual Review of Condensed Matter Physics* **15**, 131 (2024).
- [10] G. Fève, Anyon collisions and fractional statistics, in *Encyclopedia of Condensed Matter Physics (Second Edition)*, edited by T. Chakraborty (Academic Press, Oxford, 2024) pp. 402–416.
- [11] T. Chakraborty, Spin-reversed ground state and energy gap in the fractional quantum hall effect, *Surface Science* **229**, 16 (1990).
- [12] T. Chakraborty and P. Pietiläinen, Fractional quantum hall effect in tilted magnetic fields, *Physical Review B* **39**, 7971 (1989).
- [13] J. P. Eisenstein, H. L. Stormer, L. Pfeiffer, and K. W. West, Evidence for a phase transition in the fractional quantum hall effect, *Physical Review Letters* **62**, 1540 (1989).
- [14] R. G. Clark, S. R. Haynes, A. M. Suckling, J. R. Mallett, P. A. Wright, J. J. Harris, and C. T. Foxon, Spin configurations and quasiparticle fractional charge of fractional-quantum-hall-effect ground states in the $n=0$ landau level, *Physical Review Letters* **62**, 1536 (1989).
- [15] D. S. L. Abergel, V. Apalkov, J. Berashevich, K. Ziegler, and T. Chakraborty, Properties of graphene: A theoretical perspective, *Adv. Phys.* **59**, 261 (2010).
- [16] Y. Ando, Topological insulators, in *Encyclopedia of Condensed Matter Physics (Second Edition)*, edited by T. Chakraborty (Academic Press, Oxford, 2024) pp. 690–699.
- [17] P. Narang, C. A. C. Garcia, and C. Felser, The topology of electronic band structures, *Nature Materials* **20**, 293 (2021).
- [18] V. M. Apalkov and T. Chakraborty, Fractional quantum hall states of dirac electrons in graphene, *Physical Review Letters* **97**, 126801 (2006).
- [19] V. M. Apalkov and T. Chakraborty, Controllable driven phase transitions in fractional quantum hall states in bilayer graphene, *Physical Review Letters* **105**, 036801 (2010).
- [20] V. M. Apalkov and T. Chakraborty, Stable pfaffian state in bilayer graphene, *Physical Review Letters* **107**, 186803 (2011).
- [21] V. Apalkov and T. Chakraborty, Interacting dirac fermions and the rise of pfaffians in graphene, in *Encyclopedia of Condensed Matter Physics (Second Edition)*, edited by T. Chakraborty (Academic Press, Oxford, 2024) pp. 366–382.
- [22] T. Chakraborty and V. M. Apalkov, Traits and characteristics of interacting dirac fermions in monolayer and bilayer graphene, *Solid State Communications* **175–176**, 123 (2013).

- [23] X. Liu, Z. Hao, K. Watanabe, T. Taniguchi, B. I. Halperin, and P. Kim, Interlayer fractional quantum hall effect in a coupled graphene double layer, *Nature Physics* **15**, 893 (2019).
- [24] V. M. Apalkov and T. Chakraborty, Interacting dirac fermions on a topological insulator in a magnetic field, *Physical Review Letters* **107**, 186801 (2011).
- [25] A. A. Burkov, Topological properties of dirac and weyl semimetals, in *Encyclopedia of Condensed Matter Physics (Second Edition)*, edited by T. Chakraborty (Academic Press, Oxford, 2024) pp. 681–689.
- [26] H. Zheng and M. Zahid Hasan, Quasiparticle interference on type-i and type-ii weyl semimetal surfaces: a review, *Advances in Physics: X* **3**, 1466661 (2018).
- [27] A. Bernevig, H. Weng, Z. Fang, and X. Dai, Recent progress in the study of topological semimetals, *Journal of the Physical Society of Japan* **87**, 041001 (2018).
- [28] Q. Lu, P. V. S. Reddy, H. Jeon, A. R. Mazza, M. Brahlek,

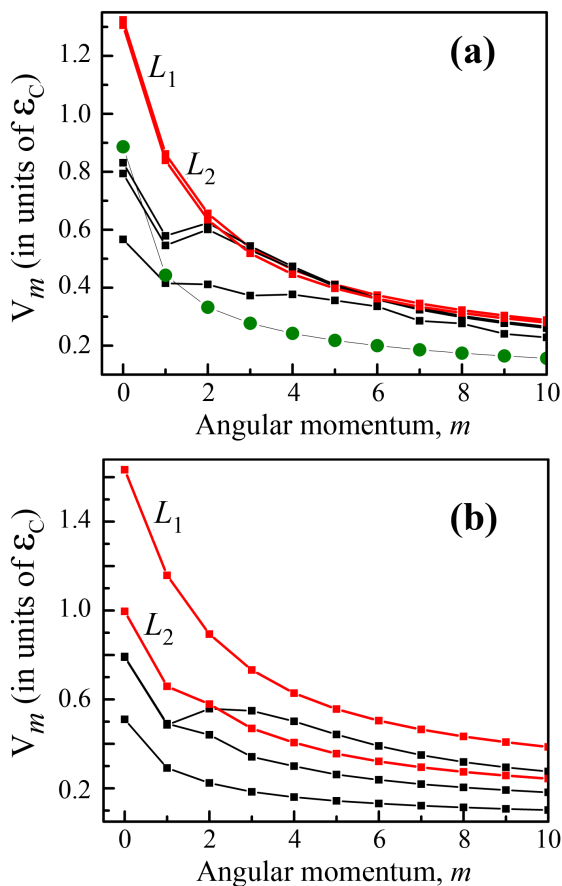


FIG. 2. Haldane pseudopotentials at a few Landau levels of a bismuthene monolayer with two values of substrate coupling, λ_S : (a) $\lambda_S = 0$, (b) $\lambda_S = \lambda_{SOC} = 55$ meV, which corresponds to the Weyl semimetal case. The largest Haldane pseudopotentials are realized at Landau levels L_1 and L_2 and are shown by red dots. The green dots in panel (a) show the Haldane pseudopotentials for a conventional electron system with parabolic energy dispersion at the $n = 0$ Landau level.

- W. Wu, S. A. Yang, J. Cook, C. Conner, X. Zhang, A. Chakraborty, Y.-T. Yao, H.-J. Tien, C.-H. Tseng, P.-Y. Yang, S.-W. Lien, H. Lin, T.-C. Chiang, G. Vignale, A.-P. Li, T.-R. Chang, R. G. Moore, and G. Bian, Realization of a two-dimensional weyl semimetal and topological fermi strings, *Nature Communications* **15**, 6001 (2024).
- [29] F. D. M. Haldane and E. H. Rezayi, Finite-size studies of the incompressible state of the fractionally quantized hall effect and its excitations, *Physical Review Letters* **54**, 237 (1985).
- [30] C. Wang, L. Gioia, and A. . Burkov, Fractional quantum hall effect in weyl semimetals, *Physical Review Letters*

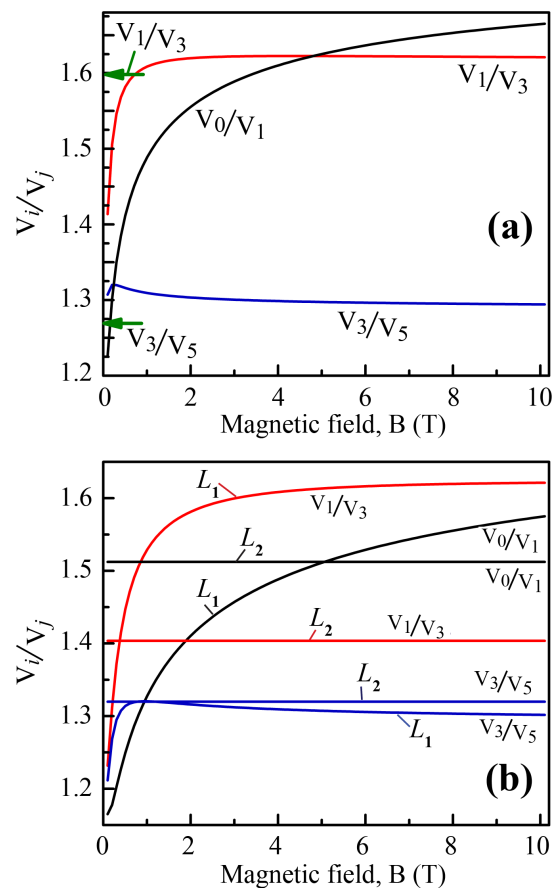


FIG. 3. Ratios of Haldane pseudopotentials V_0/V_1 , V_1/V_3 , and V_3/V_5 at L_1 and L_2 Landau levels as a function of the magnetic field are shown for a bismuthene monolayer. The value of the substrate coupling, λ_S , is $\lambda_S = 0$ (a) and $\lambda_S = \lambda_{SOC} = 55$ meV (b). In panel (a), the results for both L_1 and L_2 Landau levels are the same, while in panel (b), the data for Landau levels L_1 and L_2 are marked in the picture. Green arrows in panel (a) show the results for the case of a conventional electron system with the parabolic energy dispersion at $n = 0$ Landau level. For the case of a Weyl semimetal shown in panel (b), the ratios of pseudopotentials V_0/V_1 and V_1/V_3 for the Landau level L_2 do not depend on magnetic field.

124, 096603 (2020).

- [31] M. Thakurathi and A. A. Burkov, Theory of the fractional quantum hall effect in weyl semimetals, *Physical Review B* **101**, 235168 (2020).
- [32] J.-H. Wang, Y.-B. Yang, and Y. Xu, Fractional quantum hall effect based on weyl orbits, *Physical Review B* **111**, 045108 (2025).
- [33] J.-j. Guo, Z.-y. Luo, J.-j. Liao, Y.-z. Nie, Q.-l. Xia, R. Xiong, and G.-h. Guo, Anisotropic magnetoresistance and planar hall effect in type-ii dirac semimetal ptte2, *Journal of Applied Physics* **130**, 10.1063/5.0076675 (2021).
- [34] J. Hu, S.-Y. Xu, N. Ni, and Z. Mao, Transport of topological semimetals, *Annual Review of Materials Research* **49**, 207 (2019).
- [35] I. Mandal and K. Saha, Thermopower in an anisotropic two-dimensional weyl semimetal, *Physical Review B* **101**,

045101 (2020).

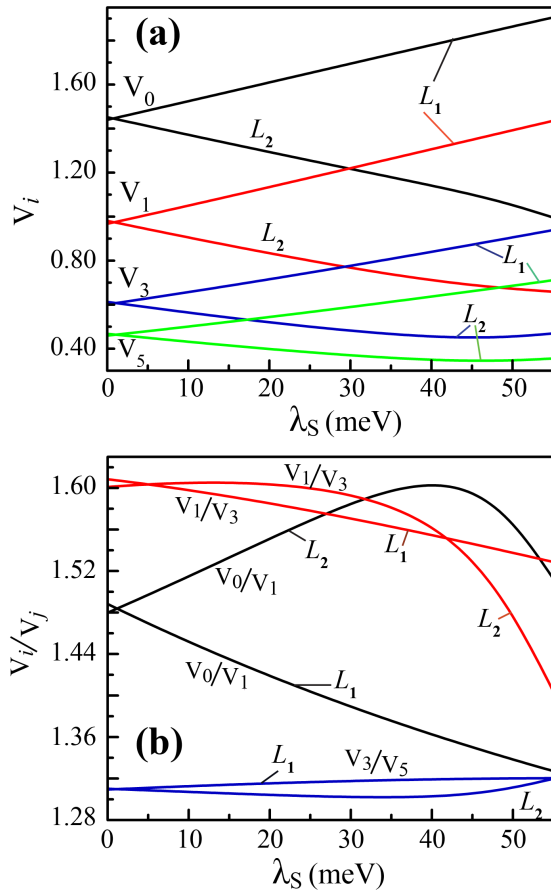


FIG. 4. Haldane pseudopotentials as a function of the substrate coupling, λ_S . The pseudopotentials are shown for two Landau levels, L_1 and L_2 . (a) The Haldane pseudopotentials $V_0, V_1, V_3,$ and V_5 are shown as a function of λ_S . (b) The ratios of the pseudopotentials, $V_0/V_1, V_1/V_3,$ and V_3/V_5 are shown as a function of λ_S . Here, $\lambda_S = 0$ corresponds to a free-standing bismuthene monolayer, while $\lambda_S = 0.055$ eV corresponds to a Weyl semimetal case. The applied magnetic field is $B = 2$ T.